Full Paper

Propellants, Explosives, Pyrotechnics

DOI: 10.1002/prep.202000270

The Diffusion of Components from Propellant and Liner at the Interfaces of EPDM Insulation

Haitao Gao,[a] Fuyin Chen,[c] Rulin Cai,[c] Sujuan Ye,[b] Feng Tan,[b] Wenjie Xiong,*[b] Yaoyong Yi,*[a] and Wei Hu*[c, d]

Abstract: The diffusion coefficient is an important parameter in the field of migration and diffusion. Different diffusion theories have been established to estimate the diffusion coefficient, including the weight gain rate. However, the research was based on the migration of different solvents into simple polymers. Few reports focused on the migration of components from propellant and liner into ethylene-propylene terpolymer (EPDM) insulation. In this paper, a new parameter named surface area diffusion rate was proposed to measure the migration of components from propellant and liner at interfaces of EPDM insulation, and the comparison with the traditional weight gain rate was made. The result shows that the surface area diffusion rate is independent of the shape of the material and is more reliable than previously used methods. Furthermore, the relationship of the surface area diffusion rate with time and temperature was investigated. In addition, the diffusion activation energy and the relationship of surface area diffusion rate with the bonding properties were discussed.

Keywords: Diffusion · Diffusion coefficient · Surface area diffusion rate · EPDM insulation

1 Introduction

Solid rocket motors are a reaction engine that in its simplest form consists of a combustion chamber, which serves as a pressure vessel and houses the propellant, non-combustible materials such as insulation (usually using ethylene-propylene terpolymer (EPDM)) to protect the combustion chamber from the extreme heat generated from the propellant combustion, and liner to bind propellant and insulation and act as stress transfer between the chamber and the propellant [1]. Inside the chamber loaded with propellant in which the most important ingredients are an oxidizer and a polymeric binder, and other additives such as plasticizer and catalysts [2]. Of the many areas of concern in the production and storability of such solid rocket motors, the major one is the adhesive bonding of propellant and liner at the interfaces of EPDM insulation, where complicated chemical and physical reactions occur, which result from the differences in the chemical composition of the insulating material and the propellant [3]. Diffusion into the insulation before the curing of the propellants is of major importance for the adhesive properties of the system [4]. Often based on the diffusion theory of adhesion, the diffusion of the component from propellant and liner at the interfaces of EPDM insulation could be predicted and desired [5]. Though the diffusion could enhance the bonding, it also changes the ratio of NCO/OH in the insulation, which could result to adhesive failure and lead to disastrous consequences [6].

Yin [7] investigated the ingredient migration and their effect in nitrate ester plasticized polyether (NEPE) propellant bonding systems by high-performance liquid chromatography (HPLC) and inductively coupled plasma spectrometer (ICP) and the results showed that the ingredient migration into the NEPE/toluene diisocyanate (TDI) liner rose with the increase of the content of the ingredient and it had no obvious disadvantageous effect on the liner storage bond property, but markedly decreased the storage mechanical property of hydroxyl-terminated poly (butadiene) (HTPB)/TDI liner and made the bond property de-

[a] *H. Gao, Y. Yi*
Guangdong Provincial Key laboratory of Advanced Welding Technology, China-Ukraine E.O.Paton Institute of Welding
No. 363 Changxing Road, Guangzhou, Guangdong, 510651, PR China
**e-mail: Yiyy@gwi.gd.cn*
[b] *S. Ye, F. Tan, W. Xiong*
National Engineering Research Center of Rubber and Plastic Sealing
Guangzhou Mechanical Engineering Research Institute Co., Ltd.
No. 2 Xinrui Road, Huangpu District, Guangzhou, 510700, PR China
**e-mail: wenjie_xiong@yeah.net*
[c] *F. Chen, R. Cai, W. Hu*
The 42nd Institute of the Fourth Academy of CASC
No. 58 Qinghe Road, Xiangyang, Hubei, 441003, PR China
**e-mail: gracehz@126.com*
[d] *W. Hu*
Songshan Lake Materials laboratory
Building A1, Innovation City, Dongguan, Guangdong Province, PR China
**e-mail: gracehz@126.com*

crease. Huang [8] qualitatively and quantitatively analysed the migration components with different boiling points in the interface of standard 25 mm cylinder specimen of NEPE propellant/liner/insulation by using gas chromatography-mass spectrometry (GCMS) and high-performance liquid chromatography (HPLC) at different experimental conditions. The results showed that the main migration components in the propellant are the plasticizers nitroglycerin (NG) and 1,2,4-butanetriol trinitrate (BTTN), and the stabilizer as well as the burning catalyst octyl dicyclopentadienyliron (ODCI), which could migrate to the liner and insulation. The main migration component is the plasticizer dioctyl sebacate (DOS), which migrates only into the insulation, not into the propellant. Gottlieb [9] studied in detail the migration of di-(2-ethylhexyl)adipate (DOA) between two propellant interfaces containing different amounts of plasticizer and between propellant and liner/insulator interfaces to correlate the physical and combustion characteristics with the migration phenomenon. Grythe [10] studied the diffusion rates in the adhesion process across the bondline between insulation and propellant in solid propellant rocket motors and evaluated the diffusion coefficients of HTPB, and glyzidyl azide polymer (GAP) in the insulation phase by the measurement of the weight of uptake method in EPDM. Plots of relative mass gain as a function of the square root of time showed good linearity up to 20–50% weight increase. The diffusion coefficients vary between 10^{-11} and 10^{-17} $m^2 s^{-1}$, which is dependent on material types and particle filling. Huang [11] found migration to appear in the interfaces of NEPE based HTPB based liner/EPDM based insulation and calculated the apparent migration activation energy (*E*a) of NG, BTTN, and a kind of aniline stabilizer in propellant, liner, and insulation, which were among 15 and 50 kJ/mol. The average diffusion coefficients were in the range of 10^{-19} to 10^{-16} $m^2 s^{-1}$.

In this paper, to overcome the deficiency of the traditional weight uptake method to evaluate the diffusion coefficients, based on Fick's law [12], a new parameter named surface area diffusion rate was proposed to measure the migration of components from propellant and liner at interface of EPDM insulation, and the comparison with the traditional weight gain rate was made. The result shows that the surface area diffusion rate is independent from the shape of the material and is more reliable. Furthermore, the relationship of the surface area diffusion rate with time and temperature was investigated. In addition, the diffusion activation energy and the relationship of surface area diffusion rate with the bonding properties were discussed.

2 Experimental Section

2.1 Material

Electronic balance (ME204E) was provided by Mettler Toledo, Switzerland with an accuracy of 0.0001 g; filter paper (Ø15 cm) was purchased from Hangzhou Special Paper Co. LTD, China and used as provided; vernier caliper was provided by Guanglu Digital Measurement Co., LTD, China with an accuracy of 0.01 mm; EPDM insulation was purchased from Jilin Chemical Industry Corporation, China and used after sulfureting; TDI with the purity of above 98.1%, isophorone diisocyanate (IPDI) with the purity of above 99% were purchased from BASF, Germany and used as provided; octyl ferrocene (OTF) with the purity of above 98%, tris-1-(2-methylaziridinyl) phosphine oxide (MAPO) with the purity of above 86% were obtained from Tanyun Technology Co., LTD, China and used as provided; hexamethylpolyisocyanate (N100) with the molecular weight of 700 Dalton, HTPB with the molecular weight of 4000 Dalton, N,N-bis-(2-hydroxypropyl)-aniline (IS211) with the purity of above 99%, nitrate ester plasticized polyether propellant A (NEPEA) with the purity of above 99%, nitrate ester plasticized polyether propellant B (NEPEB) with the purity of above 99%, ethylene oxide tetrahydrofuran copolymer (PET) with the molecular weight of 3000 Dalton, dihexyl sebacate (DHS) with the purity of above 99% and GAP with the molecular weight of 3000 Dalton were bought from Liming Research & Design institute of Chemical Industry Co. LTD, China and used as provided.

2.2 Measurement

The EPDM insulation was sliced into samples, which were labeled alphabetically, see Table 1. Then, the samples were measured accurately with the vernier caliper, weighed with the electronic balance, and then immersed in the propellant and liner with a) the component of TDI at the temperature of 25 °C to measure the different parameters of the diffusion, shown in Table 1, b) different components at different temperatures to measure the relationship of A_s with time and temperature, c) the component of the TDI at the temperature of 25 °C to measure the correlation between A_s and interface bonding property, shown in Table 7. Good surface contact between the samples and the components was ensured by sandwiching the samples between two wire sheets. The assemblies were enclosed in a sealed vessel to minimize the effect of the air and then placed in an isothermal box kept at the required temperature. Finally, the samples were taken out at set intervals, dried on a filter paper, and weighed.

2.3 Methods

The traditional weight gain rate and the weight content in the impregnation method [12] were calculated and obtained as

$$A_w = \frac{W_t - W_0}{W_0} \quad (1)$$

$$W_m = \frac{W_t - W_0}{W_t} \quad (2)$$

where the term of A_w, W_t, W_0, and W_m represents the weight gain rate, the weight of the sample at the time of t and the weight of the sample before the impregnation, and the weight content, respectively.

Based on Fick's first law [13], the diffusion flux was calculated as

$$J = -\mathrm{D}\frac{\partial c}{\partial x} \quad (3)$$

where the term of J, D, and $\partial c/\partial x$ stands for the diffusion flux, the diffusion coefficient, and the concentration gradient of the diffusion, respectively.

Provided that the immersed sample is a plane and the diffusion keeps a steady-state, the weight gain of the sample could be obtained by the following equation

$$W_t - W_0 = J \cdot S \cdot t \quad (4)$$

where the term of S and t represents the surface area of the sample and the impregnation time, respectively.

The parameter of surface area diffusion rate to illustrate the diffusion flux during a certain impregnation time is defined as follows

$$A_s = J \cdot t \quad (5)$$

where the term A_s represents the surface area diffusion rate.

According to the Arrhenius equation theory [14], the relationship of A_s with time could be fitted and illustrated as the following equation

$$A_s = A_\infty - A_1 \cdot \exp(-\frac{t}{A_2}) \quad (6)$$

where the term of t, A_1, A_2, and A_∞ stands for time, pre-exponential factor, time factor, and infinite surface area diffusion rate.

Combining equations (3) - (6), the relationship of $\ln(A_s)$ with time could be obtained as the follows

$$\ln A_s = \ln\left(-D_0 t\frac{\partial c}{\partial x}\right) - \frac{\Delta E}{R}\cdot\frac{1}{T} \quad (7)$$

where the term of D_0, $\triangle E$ and R represents coefficient, activation energy, and universal gas constant, respectively.

3 Results and Discussion

3.1 The Comparison of Different Parameters to Characterize the Diffusion

Table 1 illustrates the parameter results of the samples with different sizes after immersion in TDI for 48 hours. W_0 and W_t-W_0 increase with the increase of the sample size. The relative standard deviation (RSD) and correlation coefficient reach 71.44%, 1.0000, and 57.12%, 0.9270, respectively. This could be caused by the increase of the sample volume. However, A_w and W_m of each sample increases with the increase of the sample size. The RSD and correlation coefficient are 20.30%, −0.9297 and 16.54%, −0.9291, respectively. The large RSD and absolute value of the correlation coefficient indicate that these three parameters are heavily affected by the size of the samples. However, J and A_s of each sample varies from 0.3945 to 0.4590 and 18.93 to 22.03, respectively. And both the RSD and the correlation coefficient of J and A_s is 4.93% and 0.2813. This result explains the high consistency of J and A_s and both of them are independent of the size of the sample.

To further investigate the parameters to characterize the diffusion of TDI into the EPDM insulation, the relationship of the parameters with time at the temperature of 25 °C is studied. The results are shown in Figure 1.

It indicates that except J, the other parameters are increasing with time. Moreover, these parameters change rel-

Table 1. Results of samples with different sizes after immersion in TDI for 48 hours.

Sample	Size (mm×mm×mm)	W_0 (g)	W_t-W_0 (g)	A_w (%)	W_m (%)	J (mg/cm²·h)	A_s (mg/cm²)
A	Ø3.92×2.20	0.0274	0.0097	35.40	26.15	0.3945	18.93
B	Ø6.04×2.20	0.0650	0.0194	29.85	22.99	0.4080	19.59
C	Ø7.80×2.20	0.1083	0.0304	28.07	21.92	0.4237	20.34
D	Ø10.20×2.20	0.1851	0.0502	27.12	21.33	0.4471	21.46
E	Ø12.02×2.20	0.2570	0.0683	26.58	21.00	0.4590	22.03
F	Ø14.27×2.20	0.3623	0.0862	23.78	19.21	0.4290	20.59
G	15×10×2.30	0.3094	0.0824	26.63	21.03	0.4137	19.86
H	10×10×5.20	0.5039	0.0818	16.23	13.97	0.4177	20.05
RSD (%)		71.44	57.12	20.30	16.54	4.93	4.93
Correlation coefficient		1.0000	0.9270	-0.9297	-0.9291	0.2813	0.2813

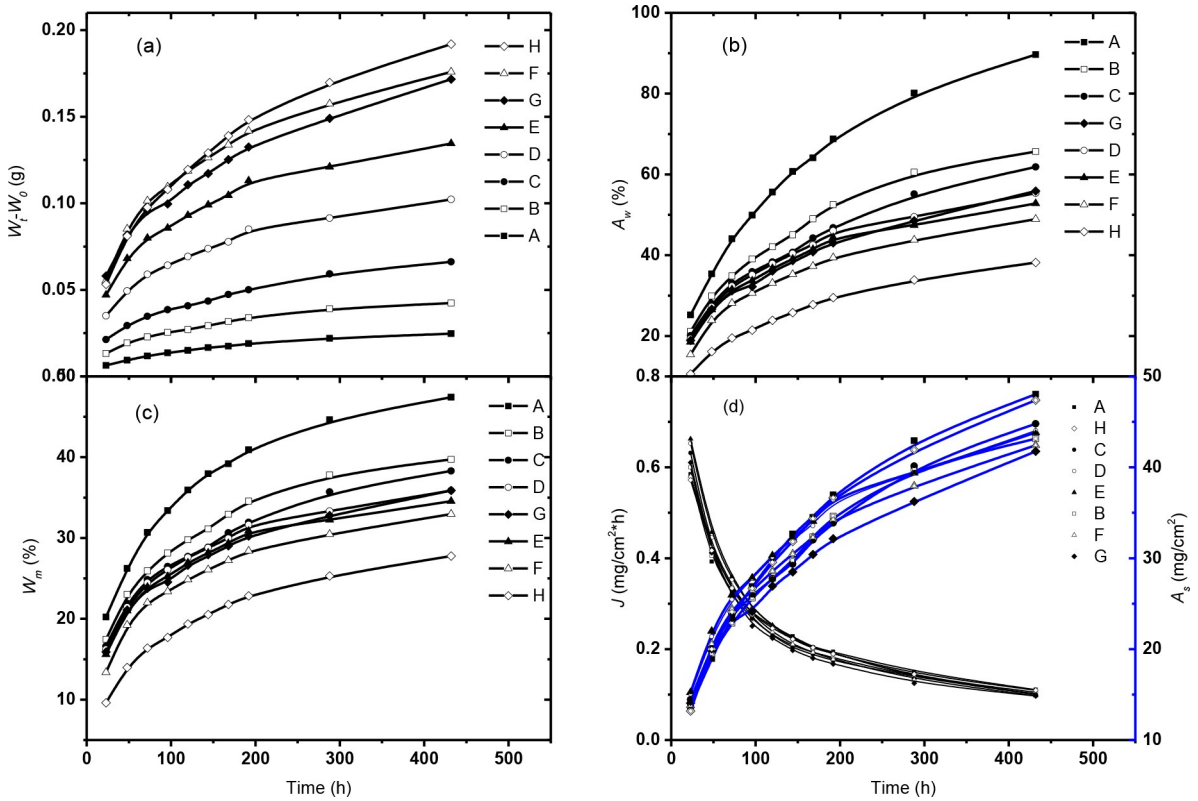

Figure 1. The relationship of (a) W_t-W_0, (b) A_w, (c) W_m, (d) J and A_s, of TDI with time.

atively fast at the early stage of the impregnation and then gradually slow down, which is in agreement with Fick's first law [13].

The RSD for each parameter at different impregnation time is listed in Table 2. It is clearly shown that the RSD of W_t-W_0, A_w, and W_m of the TDI at each impregnation time is in the range of 15.52% to 57.12%. However, the RSD of J and A_s of the TDI at each impregnation time varies between 4.26% to 5.71%. The RSD of the J and A_s of TDI at each impregnation time keeps the same because A_s is essentially the accumulation result of the J during a period of time.

Table 3 illustrates the comparison of A_w and A_s based on the data obtained from the literature [15]. It is clearly illustrated that for A_w, the relative deviation varies from 14.14% to 21.67%. However, when A_s is used as the characterization parameter, the relative deviation range is from 0.35% to 7.23%, suggesting that there is a huge decrease in terms of the relative deviation. These could be the proof that among the four parameters that could be used to characterize the diffusion property, including the traditional A_w, A_s is the most suitable parameter that is not affected by the shape of the sample and the impregnation time, to characterize the diffusion property of components from propellant and liner at the interface of EPDM insulation.

3.2 The Relationship of A_s with Time

Figure 2 illustrates the relationship of the A_s of 12 components from propellant and liner with time. It is shown that among the A_s of 12 components, 6 are positive and increase with the increase of time, while the others are negative, and decrease with the increase of time. The positives represent the diffusion and migration of the component from

Table 2. RSD for each parameter at different impregnation time.

Time/h	23	48	72	96	120	144	168	192	288	432
W_t-W_0 (g)	55.44	57.12	57.04	56.39	56.90	56.93	56.81	56.50	56.14	56.85
A_w (%)	22.68	20.30	21.51	23.06	23.63	24.47	23.99	24.32	26.11	25.67
W_m (%)	19.62	16.54	16.61	17.15	16.94	17.01	16.43	16.29	16.52	15.52
J (mg/cm^2·h)	5.71	4.93	4.38	4.49	4.41	4.97	4.26	4.92	5.32	5.09
A_s (mg/cm^2)	5.71	4.93	4.38	4.49	4.41	4.97	4.26	4.92	5.32	5.09

Table 3. A_w and A_s based on the data from the literature [15].

Parameter	Sample size (mm×mm×mm)	Time (h) 4	8	12	28	47	59
A_w (%)	10×10×2.4	2.03	2.12	2.27	2.59	3.12	3.35
	10×10×3.0	1.73	1.84	1.91	2.18	2.51	2.74
	relative deviation (%)	15.96	14.14	17.22	17.19	21.67	20.03
A_s (mg/cm^2)	10×10×2.4	16.46	17.19	18.41	21.00	25.30	27.16
	10×10×3.0	16.22	17.25	17.91	20.44	23.53	25.69
	relative deviation (%)	1.47	0.35	2.75	2.71	7.23	5.58

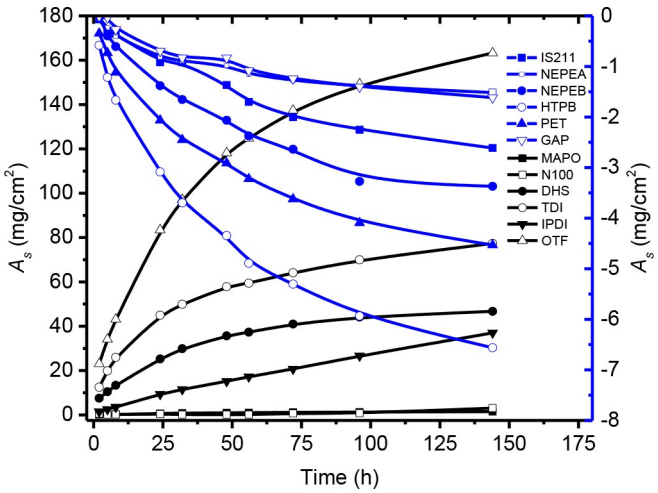

Figure 2. The relationship of A_s with time.

propellant and line to the insulation, and the negatives means the diffusion and migration of the component from the insulation to the propellant and liner. The positive ones correspond to OTF, TDI, DHS, IPDI, MAPO, N100, and the negative ones correspond to HTPB, PET, NEPEB, IS211, NEPEA, GAP, respectively. It is not neglectable that the A_s of N100 and MAPO is nealy zero and stays unchanged. The reasons could be related to the molecular structure of the component. OTF, TDI, DHS, IPDI, MAPO are made up of small molecules, except N100, while HTPB, PET, NEPEB, IS211, NEPEA, GAP are composed of polymer compounds or consist of polymer mixture. Therefore, it could be concluded that when the insulation bonds or contacts with the propellant and liner, whether the diffusion or migration occurs by means of the component from the propellant and liner to the insulation or the other way around depends on the molecular structure of the component. When the component is composed of polymer, the component migrates from the propellant and liner to the insulation. And when it is made up of small molecules, the component migrates from the insulation into the propellant and liner.

Table 4 shows the results of the parameters of the functions after fitting the curves with an exponential function in Figure 2. A_s the MAPO and the N100 are almost zero in the range of 144 hours, the fittings with the expaonential function are meaningless and thus could be ignored. The correlation coefficients of the curves are all above 0.99, except that of the GAP. This further illustrates that the relationship of A_s with time fits the exponential function well and that the diffusion behavior agrees well with the same dynamic model.

Table 4. The parameters of the functions.

Components	A_∞	A_1	A_2	R
DHS	47.12	41.60	37.32	0.9998
TDI	75.35	63.87	37.46	0.9952
IPDI	87.11	85.94	273.35	0.9990
OTF	165.87	148.54	42.83	0.9996
IS211	−3.15	−3.13	79.18	0.9953
NEPEA	−1.50	−1.47	38.38	0.9904
NEPEB	−3.59	−3.58	52.39	0.9980
HTPB	−6.79	−6.27	47.73	0.9983
PET	−4.73	−4.42	51.13	0.9980
GAP	−1.66	−1.76	50.08	0.9878

3.3 The Relationship of A_s with Temperature

Figure 3 gives the illustrations of the relationship of A_s with temperature within 24 hours for the components. It is clearly shown that the absolute value of A_s increases with the increase of temperature.

Figure 4 illustrates the relationship of A_s with time under different temperatures, of the TDI, IPDI, DHS, and OTF, respectively. It is easily noticed that under the temperature of 60 °C, A_s increases with the increase of time and each of the curves gets a similar exponential changing trend. In addition, the surface area diffusion rate increase with the increase of the temperature. However, when the temperature reaches 70 °C, the curves of the TDI and IPDI derive significantly from the predicted normal state, which is clearly illustrated by the phenomenon that the curves of the TDI and IPDI at the temperature of 70 °C obtain crossings with the curves at lower temperatures and that A_s of the TDI decreases with the increase of time at the temperature of 70 °C. These could result from the facts that at the temperature of 70 °C, the physical or chemical properties of the TDI and the IPDI or of the insulation changes, such as chemical reaction occur between the TDI or the IPDI with the in-

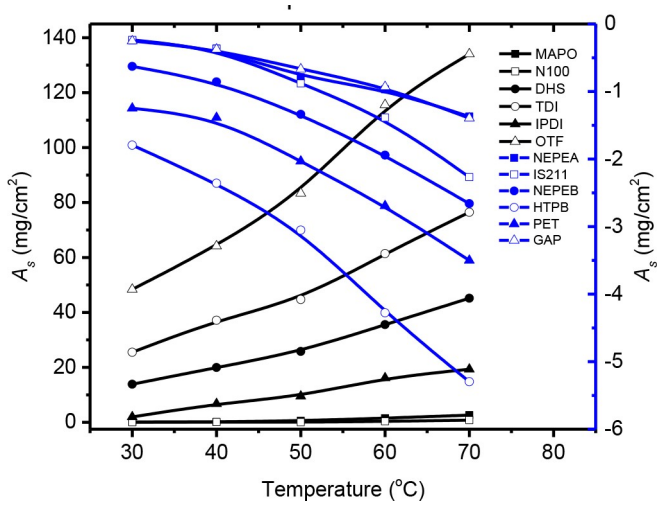

Figure 3. The relationship of A_s from temperature within 24 hours.

sulation to change the chain structure or the system morphology, which could determine the diffusion properties of the system [16].

To illustrate the relationship of the parameters of the fitting exponential function with the temperature, the parameters of the DHS and OTF were calculated shown in Table 5. The A_∞ represents A_s when the diffusion reaches equilibrium after infinite time at certain temperature. It is clearly shown that the correlation coefficient of the curves are above 0.99, which means the curves fit well with the measured data. The A_∞ of both DHS and OTF increases as the temperature rises, which means the increasing temperature could enhance the diffusion of the component to the insulations.

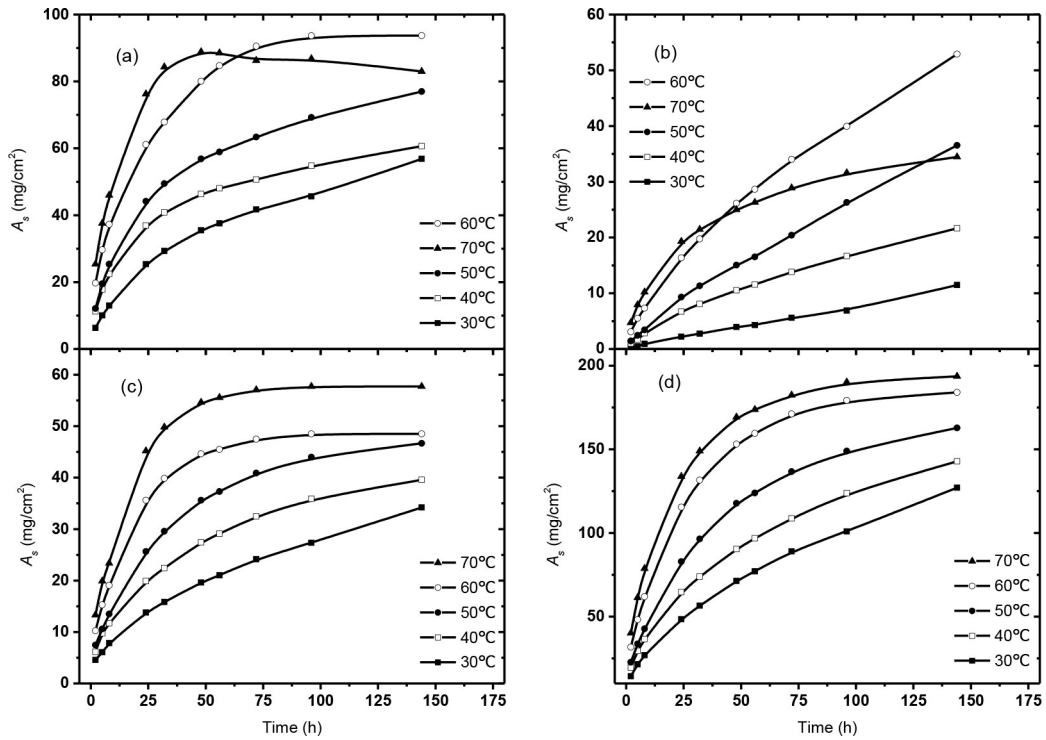

Figure 4. The relationship of the A_s of the (a) TDI, (b) IPDI, (c) DHS, and (d) OTF, with time.

Table 5. The calculated parameters of fitting exponential funtion of the DHS and OTF.

Temperature (°C)	DHS				OTF			
	A_∞	A_1	A_2	R	A_∞	A_1	A_2	R
30	40.88	36.52	90.59	0.9982	155.27	141.02	93.91	0.9985
40	41.15	35.26	50.74	0.9989	155.16	136.52	64.25	0.9989
50	47.12	41.60	37.32	0.9998	165.87	148.54	42.83	0.9996
60	48.44	42.58	20.47	0.9998	184.17	162.47	28.57	0.9999
70	57.63	50.08	17.66	0.9998	191.70	161.86	23.86	0.9994

3.4 The Activation Energy of the Diffusion

Figure 5 illustrates the relationship of $\ln(A_s)$ with $1/T$, of the DHS, TDI, IPDI, and OTF, respectively. It is clearly shown that the $\ln(A_s)$ decreases with the increase of $1/T$ and at each set $1/T$, the $\ln(A_s)$ of the OTF is the biggest. $\triangle E$ could be obtained from the intercept of the fitted line. Thus, $\triangle E$ of each component was calculated as shown in Table 6.

The magnitude of $\triangle E$ reveals the ability of the component from propellant and liner to diffuse. The larger the activation, the easier the component diffuses and the easier the insulation absorbs the component. The result in Table 6 indicates that each $\triangle E$ of the four components varies from 22.6 kJ/mol to 46.3 kJ /mol. The order of diffusion ability from large to small is the IPDI > DHS > TDI > OTF, which agrees well with the opposite order of diffusion amount of each component to the insulation, and thus, this infers that $\triangle E$ is the internal factor that controls the diffusion and migration of the component to the insulation.

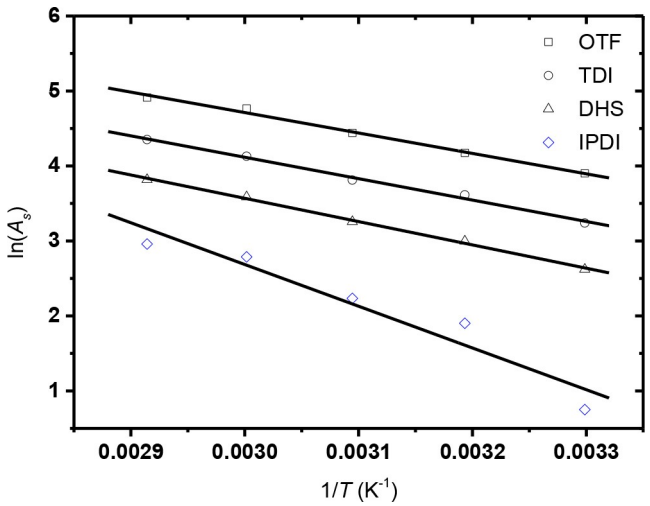

Figure 5. The relationship of $\ln(A_s)$ with $1/T$.

Table 6. The activation energy of each four components.

Component	DHS	TDI	IPDI	OTF
$\triangle E$ (kJ/mol)	25.7	23.5	46.3	22.6

3.5 The Relationship of A_s with the Interface Bonding Property

Table 7 illustrates the relationship of A_s with the bonding property obtained at different impregnation time. The RSD of each kind is approximately 15 %, suggesting that the discrepancies of RSD results in different type samples are derived from the discrepancies of the property of the samples. By qualitative analysis, based on the probabilities of interface debonding, which is difficult to characterize quantitatively, the bonding property of the samples is roughly classified into better, moderate, and poor. The result indicates that the samples with relatively high A_s have better interface bonding property, and the samples with relatively poor bonding property have lower A_s. This could be concluded that the parameter of A_s has some correlation to the interface bonding property. Although such correlation and mechanism is not clear at present, it offers the direction that needs further investigation in future work.

4 Conclusion

The parameter A_s was proposed to characterize the diffusion of the components from propellant and liner at the interfaces of EPDM insulation. The result shows that it is independent of the sample size and is a more suitable parameter to characterize the diffusion phenomenon compared with the traditional parameters. To further investigate the diffusion from propellant and liner at the interfaces of EPDM insulation, 12 different kinds of components of propellant and liner were studied. The fittings of the curves match well with the function of $A_s = A_\infty - A_s \cdot \exp(-t/A_s)$. $\triangle E$ of four components varies from 22.6 kJ/mol to 46.3 kJ/mol. The parameter of A_s is related to the interface bonding property and the mechanism will be investigated in future work.

Acknowledgements

This work was supported by the GDAS Special Project of Science and Technology Development (2020GDASYL-20200402006, 2020GDASYL-2020103123, 2020GDASYL-20200301001, 2018GDASCX-0802), Guangzhou Science, Technology Project

Table 7. The relationship of A_s with the interface bonding property under the temperature of 25 °C.

Type	Bonding property	Time (h) 25	48	72	96	120	144	241	384
a	moderate	13.10	18.40	22.86	26.35	29.02	32.09	38.43	44.91
b	better	16.44	22.78	27.97	32.86	37.02	40.91	48.30	55.64
c	better	14.44	20.14	24.92	28.84	31.60	34.53	39.97	46.61
d	poor	11.41	15.87	20.05	23.37	26.06	28.68	33.91	39.38
e	poor	11.47	16.37	20.12	23.01	25.59	27.98	33.15	38.79
RSD (%)		15.92	15.16	14.50	15.24	15.68	15.93	15.67	15.13

(201807010029, 201807010028) and National Key R&D Program of China (2017YFB0305700, 2018YFB2001002) and the Program of Guangdong Introducing Innovative and Enterpreneuial Teams (2019BT02Z393).

Data Availability Statement

No data available.

References

[1] M. S. Sureshkumar, C. M. Bhuvaneswari, S. D. Kakade, M. Gupta, Studies of the properties of EPDM-CSE blend containing HTPB for case-bonded solid rocket motor insulation, *Polym. Adv. Technol.* **2009**, *19*, 144–150.

[2] L. Gottlieb, S. Bar, Migration of Plasticizer between Bonded Propellant Interfaces, *Propellants Explos. Pyrotech.* **2003**, *28*, 12–17.

[3] K. F. Grythe, F. K. Hansen, H. Walderhaug, NMR Self-Diffusion and Viscosity of Polyurethane Formulations for Rocket Propellants, *J. Phys. Chem. B* **2004**, *108*, 12404–12412.

[4] A. V. Pocius, *Adhesion and Adhesives Technology: An Introduction*, Carl Hanser Verlag GmbH & Co. KG, New York, USA, **2012**.

[5] a) H. L. Schroeder-Gibson, Adhesion of solid rocket materials, *Rubber World*, **1990**, *11*, 928–931; b) B. Han, Y. T. Ju, C. S. Zhou, Simulation of crack propagation in HTPB propellant using cohesive zone model, *Eng. Fail. Anal.* **2012**, *26*, 304–317; c) H. R. Cui, G. J. Tang, Z. B. Shen, A three-dimensional viscoelastic constitutive model of solid propellant considering viscoelastic Poisson's ratio and its implementation, *Eur. J. Mech. A/Solid.* **2017**, *61*, 235–244; d) A. M. Jiang, G. C. Li, W. D. Huang, X. Qiu, Experimental and Numerical Simulation on Deformation and Debonding Processes of HTPB Propellant/Liner Adhesive Specimen, *Acta. Armam.* **2014**, *35*, 1619–1624; e) W. Zhu, D. M. Liu, J. J. Xiao, X. H. Chi, A. M. Pang, H. M. Xiao, Molecular dynamics simulations of the structures and properties of NEPE propellant/liner (I) – Illustrating curing reactions and comparing mechanical properties of the simplified models, *J. Solid Rocket Techno.* **2014**, *37*, 530–534; f) W. Zhu, D. M. Liu, J. J. Xiao, X. H. Chi, A. M. Pang, H. M. Xiao, Molecular dynamics simulations of the structures and properties of NEPE propellant/liner (II) – Demonstrating component molecule migrating and formulation for complex system, *J. Solid Rocket Techno.* **2014**, *37*, 678–683.

[6] K. F. Grythe, *Study of the Interface between Insulation and Propellant in Solid Propellant Rocket Motors*, NTNU: Trondheim, Norway **2002**.

[7] H. L. Yin, Y. Wang, D. F. Li, Ingredient migration and their effect on NEPE propellant bonding system, *J. Solid Rocket Techno.* **2009**, *32*, 527–530.

[8] a) Z. Huang, J. Liu, S. Xu, J. Bai, X. Ma, Qualitative analysis of migration components in the interface of NEPE propellant, *J. Solid Rocket Techno.* **2010**, *33*, 541–544; b) Z. Huang, L. Tan, Q. Cao, X. Ma, Quantitative analysis of Migrating Components in Interface of NEPE Propellant/Liner/Insulation, *Chin. J. Energet. Mater.* **2010**, *18*, 330–334.

[9] L. Gottlieb, S. Bar, Migration of Plasticizer between Bonded Propellant Interfaces, *Propellants Explos. Pyrotech.* **2003**, *28*, 12–17.

[10] K. F. Grythe, F. K. Hansen, Diffusion Rates and the Role of Diffusion in Solid Propellant Rocket Motor Adhesion, *J. Appl. Polym. Sci.* **2007**, *103*, 1529–1538.

[11] Z. P. Huang, H. Y. Nie, Y. Y. Zhang, L. M. Tan, H. L. Yin, X. G. Ma, Migration kinetics and mechanisms of plasticizers, stabilizers at interfaces of NEPE propellant/ HTPB liner/EDPM insulation, *J. Hazard. Mater.* **2012**, *229–230*, 251–257.

[12] H. Xu, S. N. Wang, J. M. Zheng, Description of the diffusion phenomenon using free volume theory. *Chin. J. Pharmaceut.* **2004**, *2*, 7–11.

[13] a) J. Comyn, *Polymer Permeability*, Chapter 1: Introduction to Polymer Permeability and the Mathematics of Diffusion, Leicester Polytechnic, UK, **1985**; b) Y. H. Kong, Z. R. Liu, C. M. Yin, C. Y. Wu, A New Method Rapidly Measuring Nitroglycerin in the Coating of the Rocket Propellant, *Propellants Explos. Pyrotech.* **1989**, *14*, 212–214.

[14] H. L. Lv, B. Q. Wang, Diffusion coefficients in polymer-solvent systems—Vrentas-Duda's model and its development. *J. Funct. Polym.* **2005**, *18*, 353–360.

[15] Y. Zhang, X. H. Wang, F. Q. Zhao, The testing method study on the migration of nitroglycerine to the coating. *Explos.* **1993**, *3*, 39–43.

[16] Y. S. Tung, R. Mu, D. O. Henderson, W. A. Curby, Diffusion Kinetics of TNT in Acrylonitrile-Butadiene Rubber via FT-IR/ATR Spectroscopy. *Appl. Spectrosc.* **1997**, *51*, 171–177.

Manuscript received: October 11, 2020
Revised manuscript received: November 5, 2020
Version of record online: January 29, 2021

